Doppler Spectrum from Moving Scatterers in a Random Environment

Andersen, Jørgen Bach; Nielsen, Jesper Ødum; Pedersen, Gert Frølund; Bauch, Gerhard; Dietl, Guido

Published in:
IEEE Transactions on Wireless Communications

DOI (link to publication from Publisher):
10.1109/TWC.2009.081088

Publication date:
2009

Document Version
Early version, also known as pre-print

Doppler Spectrum from Moving Scatterers in a Random Environment

Jørgen Bach Andersen, *Life Fellow, IEEE*, Jesper Ødum Nielsen,
Gert Frølund Pedersen, Gerhard Bauch, *Senior Member, IEEE*, Guido Dietl, *Member, IEEE*

***Abstract*—A random non-line-of-sight environment with stationary transmitter and receiver is considered. In such an environment movement of a scatterer will lead to perturbations of the otherwise static channel with a resulting Doppler spectrum. This is quite a general situation in outdoor environments with moving traffic or indoor situations with moving people. Here we study the latter situation in detail with experimental results from a large office environment. A general theory of Doppler spectra is developed. The impact of a scatterer depends on the angular distribution of scattered energy, and uniform as well as sharply peaked distributions are considered in the theory. The Doppler spectra are in all cases sharply peaked at zero frequency due to forward scattering, but the actually measured distribution depends on the degree and type of activity in the environment, as well as the spectrum estimation accuracy.**

***Index Terms*—Indoor propagation, small terminal antennas, radio channel, user influence**

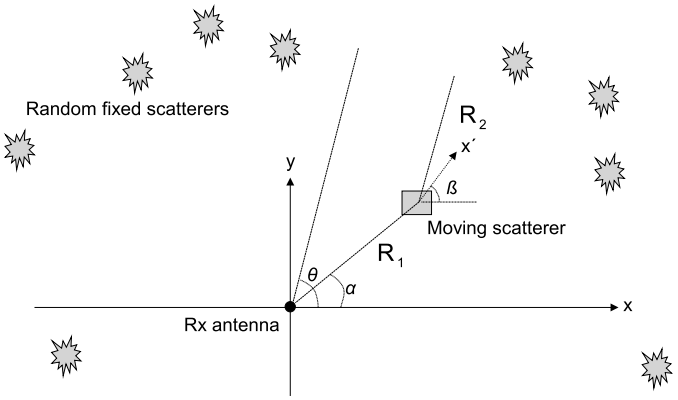

Fig. 1. Geometry of the situation with fixed random scatterers and a moving external scatterer.

I. Introduction

Doppler spectra are important for the determination of the time variance of the wireless channels. The usual situation is the one with a moving antenna in a random environment leading to the classical Jakes spectrum for scatterers uniformly distributed in azimuth. In some cases the antenna is stationary and the variance of the channel is created by the movement of external scatterers, being it from vehicles in an outdoor environment or from persons in an indoor environment. It is this latter case we are treating in this paper. Early experimental work in this area [1], [2] shows a spectrum which peaks at 0 Hz and falls off rapidly, but no theory is provided. Theoretical results are given in [3], but only for the case of small scatterers with uniform scattering pattern, and the equation for the Doppler spectrum is incorrect, although the equation for the correlation is correct. It is interesting, but not surprising, that the situation of two vehicles moving in a random environment is similar to the one here with fixed terminals and moving scatterers, so the basic analysis of the Doppler spectrum may also be found in [4], [5], for the case of equal velocity of the two vehicles.

The paper is organized as follows. The theoretical cases are treated in Section II, where a distinction is made for different scattering patterns from the moving scatterers, which have a significant impact on the Doppler spectra. Analytical solutions are given where possible. Section III describes the indoor measurement setup and the environment with moving or stationary users. The data processing and results are discussed in Section IV and V, respectively.

J. Bach Andersen, J. Ødum Nielsen, and G. Frølund Pedersen are with the APNet section at the Department of Electronic Systems, Aalborg University, Denmark. G. Dietl is with DoCoMo Euro-Labs, Munich, Germany. G. Bauch is with DoCoMo Euro-Labs and Universität der Bundeswehr München, Germany.

II. Theory

The geometry and situation is shown in Fig. 1. A number of fixed, but random scatterers surround the antenna which is also fixed. The scatterers are assumed to be illuminated by some external source and rescatter the energy towards the antenna. They also illuminate the moving scatterer, so the antenna receives two sets of signals, one directly from the scatterers and one indirectly via the moving scatterer.

The angles are defined as follows: θ is the angle to a fixed scatterer assumed to be in the far field, α the angle towards a moving scatterer, and β the angle of the direction in which the scatterer is moving (x' direction).

A. Moving Antenna

Let us first review the classical situation with a moving antenna for easy reference. In the narrowband case the spatial variation is modeled as

$$h(x) = \sum_{i=1}^{I} a_i e^{j2\pi x \cos(\theta_i)} \tag{1}$$

where a_i is the complex magnitude of the i-th scatterer, and θ_i the angle towards the scatterer measured from the x-axis, the direction of movement. I is the number of scatteres. The complex magnitudes are assumed to be uncorrelated complex Gaussians with mean power of 1 corresponding to a uniform distribution of scatterers. Distance is measured in

Published in *IEEE Transactions on Wireless Communications, Vol. 8, No. 6, pp 3270-3277, June 2009.* DOI:10.1109/TWC.2009.081088

wavelengths. In order to find the spectrum we first derive the autocorrelation $R(\Delta)$, which is the inverse Fourier transform of the spectrum and where Δ is the incremental value in distance. By straightforward calculations we find

$$R(\Delta) = \mathrm{E}\{h(x)h^*(x+\Delta)\} \tag{2}$$

$$= \frac{1}{2\pi}\int_0^{2\pi} e^{j2\pi\Delta\cos(\theta)}\,d\theta = J_0(2\pi\Delta) \tag{3}$$

$$S(u) = \int_{-\infty}^{\infty} e^{jut}J_0(t)\,dt = \frac{2}{\sqrt{1-u^2}}, \qquad u^2<1 \tag{4}$$

where $\mathrm{E}\{\cdot\}$ denotes statistical expectation, $J_0(\cdot)$ denotes the Bessel function of 0-th order, and $S(u)$ is the spatial Doppler spectrum, the familiar "bathtub" case [6]. In the continuous version it is assumed that the number of scatterers is infinite. All lengths have been normalized to the wavelength and $u=1$ corresponds to the maximum Doppler shift. In standard terminology $u=1$ corresponds to a Doppler frequency $f_D = v/\lambda$ with v the velocity and λ the wavelength.

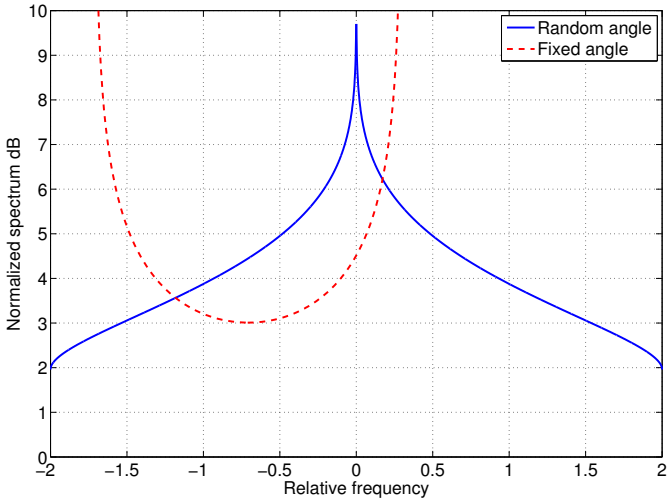

Fig. 2. Dashed line: Doppler spectrum from a moving scatterer at an angle of $\beta = 45°$ with zero direct field at antenna. Uniform scattering pattern. Solid line: Same averaged over all angles, the 'Akki' spectrum [4].

B. Moving Scatterer

R_1 is the distance to the moving scatterer and R_2 is the distance from the moving scatterer to the fixed scatterer. The relevant phase change is the electrical length of the distance $s = R_1 + R_2$ as a function of x'. The angle of the direction of movement is β. Simple geometric considerations lead to the following

$$R_1 = R_1^0 + x'\cos(\beta-\alpha) \tag{5}$$

$$R_2 = R_2^0 - x'\cos(\beta-\theta) \tag{6}$$

$$\phi = k(R_1+R_2) \tag{7}$$

$$= k(R_1^0+R_2^0) + kx'\left[\cos(\beta-\alpha)-\cos(\beta-\theta)\right] \tag{8}$$

where $k = 2\pi/\lambda$ is the wavenumber and where R_1^0 and R_2^0 are the initial distances. The spatial Doppler shift, the derivative of phase ϕ, is then

$$f_D = \frac{\partial\phi}{\partial x'} = 2\pi\left[\cos(\beta-\alpha)-\cos(\beta-\theta)\right] \tag{9}$$

with all distances measured in wavelengths. The total transfer function from the i-th scatterer is then

$$H_i(x') = a_i + \sqrt{P_i(\theta_i-\alpha_i)}e^{-j2\pi x'[\cos(\beta_i-\alpha_i)-\cos(\beta_i-\theta_i)]} \tag{10}$$

where a_i is the direct field at the antenna and P_i the scattered power, equal to the bistatic radar cross-section of the scatterer. The bistatic radar cross section [7] is defined as

$$P_i(\theta_i-\alpha_i) = 4\pi d^2\frac{S_{\mathrm{sc}}(\alpha_i)}{S_{\mathrm{in}}(\theta_i)} \tag{11}$$

where d is the distance from the scatterer, $S_{\mathrm{in}}(\theta_i)$ the incident power density, and $S_{\mathrm{sc}}(\alpha_i)$ the scattered power flux density. The radar cross section depends very much on the electrical size of the scatterer as will be discussed later. It is assumed that P_i is independent of β and that the mean value of the power from each fixed scatterer is unity. With these assumptions the correlation function is

$$R(\Delta) = \sum_{i=1}^{I} P_i(\theta_i-\alpha_i)e^{-j2\pi\Delta[\cos(\beta_i-\alpha_i)-\cos(\beta_i-\theta_i)]} \tag{12}$$

$$= \iiint_0^{2\pi} P(\theta-\alpha)e^{-j2\pi\Delta[\cos(\beta-\alpha)-\cos(\beta-\theta)]}\,d\beta\,d\alpha\,d\theta \tag{13}$$

assuming a continuous distribution of scatterers. Δ is the spatial variable in wavelengths. In both (12) and (13) the contribution from the constant field is omitted. In the general case numerical simulations are necessary, but some special cases are worth discussing.

C. Single scatterer with constant scattering cross section, moving in one direction

Without loss of generality the single scatterer may be positioned along the x-axis so $\alpha = 0$. For a constant scattering cross section $P = 1$ and for fixed β we find for a uniform distribution of θ over 2π

$$R(\Delta) = \frac{1}{2\pi}\int_0^{2\pi} e^{-j2\pi\Delta[\cos(\beta)-\cos(\beta-\theta)]}\,d\theta \tag{14}$$

$$= e^{-j2\pi\Delta\cos(\beta)}J_0(2\pi\Delta) \tag{15}$$

$$S(u) = \frac{2}{\sqrt{1-\left[\cos(\beta)+u\right]^2}} \tag{16}$$

The case of uniform scattering will be approximately satisfied for electrically small scatterers, like rain drops or leaves, assuming dimensions less than a wavelength. The result is surprisingly simple. The spectrum shape is the same for the scatterer as for the moving antenna, but shifted, with the peaks at $u = 1-\cos(\beta)$ and $u = -1-\cos(\beta)$. An example of a spectrum for $\beta = 45°$ is shown in Fig. 2. In case the direct field is non-zero a δ-function should be added at $u = 0$. Note that this value is in itself an exponentially distributed random number.

Published in *IEEE Transactions on Wireless Communications, Vol. 8, No. 6, pp 3270-3277, June 2009.* DOI:10.1109/TWC.2009.081088

D. Single scatterer with constant scattering cross section, moving in many directions

In this case the direction β is also a random variable with uniform distribution over 2π, the result is again a Bessel function so the final correlation is

$$R(\Delta) = J_0^2(2\pi\Delta) \tag{17}$$

This agrees with the result in [4]. In fact it may be noted that it is the effect of the difference between two random cosines, and this may be achieved in several other situations, like random positions of fixed scatterers and random scatterers, or random positions of many scatterers moving in random directions, even for LOS (one fixed scatterer).

The mean spectrum, the Fourier transform of the correlation, has an analytical solution [4],

$$S(u) = \frac{1}{\pi^2} K\left[\sqrt{1-\left(\frac{u}{2}\right)^2}\right] \tag{18}$$

where $K[\cdot]$ is the elliptic integral of the first kind. The spectrum is also shown in Fig. 2 and is peaked at zero frequency with a logarithmic singularity and otherwise rather flat. It is interesting that there is a peak at zero frequency even for no direct field at the antenna. It will be apparent later (*e.g.*, Fig. 7) that this distribution does not agree with our experimental results.

E. Non-uniform scattering pattern

In the previous sections the scattering was assumed to be evenly distributed in azimuth. This is a convenient assumption, but unrealistic, especially for an electrically large scatterer such as a human body, where the scattering pattern will be peaked in the forward direction. The physical reason for the large forward scatter is the small total field in the shadow region, where the total field is the sum of the incident and the scattered field, and the latter two have approximately opposite sign behind the scatterer.

Fig. 3 shows a theoretical two-dimensional case for scattering around a conducting cylinder of radius 20 cm at a distance of 60 cm as a function of angle. The incident field comes from direction $\phi = 0^\circ$, so the forward scattering direction is $\phi = 180^\circ$. It is noted that the scatterer diminishes the total field in the shadow region (same as the forward scattering region), while the scattered field peaks in this direction. The calculations are based on Bessel function expansions of the incident and scattered fields [7].

The extreme case of a narrow scattering pattern is a delta function, $P(\theta-\alpha) = \delta(\theta-\alpha)$, leading to $R(\Delta)$ equal to a constant, and the spectrum $S(u) = \delta(u)$. So there is a strong correlation between the shape of the scattering pattern and the Doppler spectrum. From a numerical point of view it is convenient to make a Fourier transform of the scattering

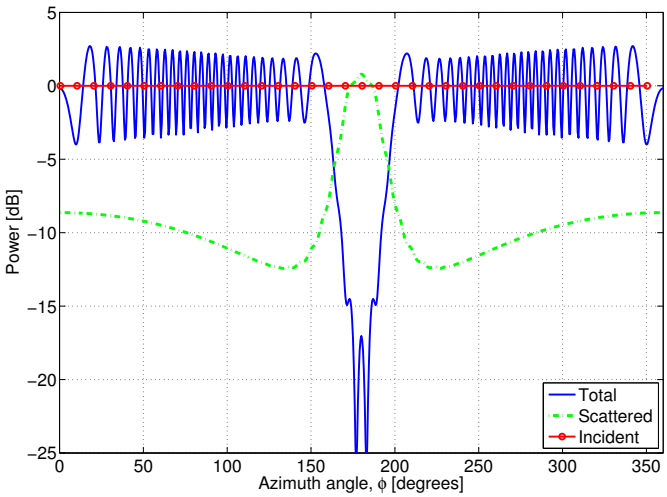

Fig. 3. Two-dimensional scattering around a conducting cylinder of radius 20 cm at 6 GHz with electric field along the axis. The incident field is a plane wave from direction $\phi = 0^\circ$ and the observation radius is 60 cm. The forward scattering direction corresponds to $\phi = 180^\circ$. The peaking of the scattered field and the shadowing of the total field is apparent in the forward scattering direction.

pattern

$$P(\gamma) = \sum_{n=0}^{\infty} b_n \cos(n\gamma) \tag{19}$$

$$R(\Delta) = \sum_{n=0}^{\infty} b_n R_n(\Delta) \tag{20}$$

$$S(u) = \sum_{n=0}^{\infty} b_n S_n(u) \tag{21}$$

taking advantage of the theoretical results for the correlation and the spectrum,

$$R_n(\Delta) = \frac{1}{(2\pi)^2}\int_0^{2\pi} d\beta \int_0^{2\pi} d\theta\, \cos(n\theta) e^{j2\pi\Delta[\cos(\beta-\theta)-cos(\beta)]} \tag{22}$$

$$= J_n^2(2\pi\Delta) \tag{23}$$

$$S_n(u) = \int_{-\infty}^{\infty} J_n^2(2\pi\Delta) e^{j2\pi\Delta u} d\Delta = (-1)^n P_{n-0.5}\left(\frac{u^2}{2}-1\right) \tag{24}$$

where J_n and P_n are the n-th order Bessel and Legendre functions, respectively [8], and γ is the angle measured from the forward direction. It should be noted that non-integer orders of the Legendre functions are needed in (24), which is not directly supported by, *e.g.*, Matlab. In practice it may be easier to obtain the spectrum via a discrete Fourier tranform of (20).

For comparison with the experiments described later we have chosen a smooth scatter pattern mimicking the measured smooth spectra, and found that the following is a good model,

$$P(\gamma) = \frac{1}{\gamma^2 + a} \tag{25}$$

where a is a constant. For a particular case, shown in Fig. 4, $a = 0.02$ is chosen.

Fig. 4 compares a measurement result with the theory, showing the significance of the scattering pattern. The measurement

Published in *IEEE Transactions on Wireless Communications, Vol. 8, No. 6, pp 3270-3277, June 2009.* DOI:10.1109/TWC.2009.081088

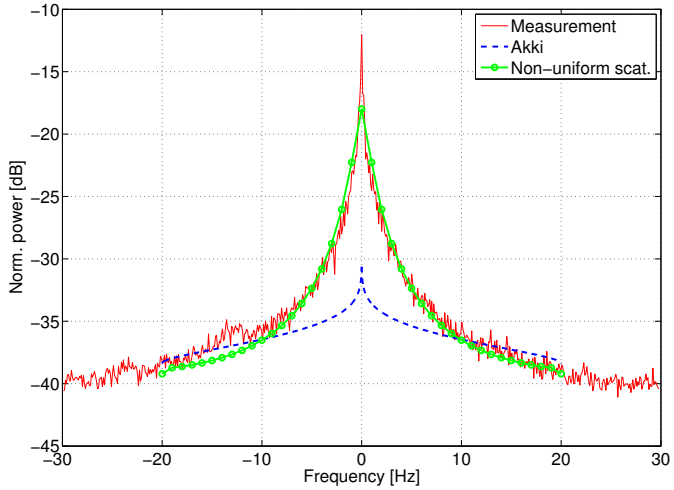

Fig. 4. Doppler spectra for a typical experimental case (solid line), a model fit based on the scattering pattern in Equation (25) (solid line with circles), and the 'Akki' spectrum for uniform scattering (dashed curve). The curves are vertically positioned arbitrarily, and the model is scaled with frequency to make a good fit.

is described below in Section III, and is one ('R1, Free') of several shown in Fig. 7. For the comparison, the curves are shifted vertically (it is a dB scale) and the frequency axis is stretched to make a best fit. Since the theoretical spectrum is limited to the maximum Doppler frequency, it is interesting to note that the maximum seems to be around 20 Hz corresponding to a maximum speed of 0.5 m/s, which seems reasonable.

III. Measurements

The measured data used in the current work is obtained using a multiple-input multiple-output (MIMO) channel sounder operating at a carrier frequency of 5.8 GHz. The sounder uses the correlation principle, and measures 16 transmit channels simultaneously, where each transmit branch uses a 1 W power amplifier. On the receive side eight channels were measured in parallel, and using 1:4 switching each branch is extended so that in total 32 receive channels are measured. Additional information about the sounder is available in [9]. The full complex 16×32 MIMO channel is measured in a time-triggered way at a rate of 60 Hz. In a post-processing procedure the measurements are compensated for the sounder system response and the bandwidth is limited to about 100 MHz. The compensation removes differences from the desired system response, taking into account the frequency dependent amplitudes and phases for all combinations of Tx and Rx branches.

The measurements were made on the down-link (DL) using two access points (AP's) each with 8 elements arranged in a circle and mounted on a wooden pole at about 2.1 m above the floor, close to the ceiling. AP1 denotes the array located near the middle of the room, while AP4 was near one of the end walls, see Fig. 5. In the figure the dashed lines indicate light partitions of height about 1.8 m and the double lines indicate wooden bookshelves which are standing on the floor and of the same height as the partitions. Although the AP's are higher than the partitions not all of the mobile station (MS) positions have optical view of the AP's.

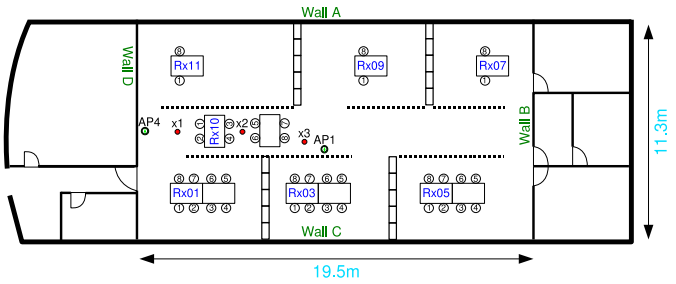

Fig. 5. Overview of measurement site.

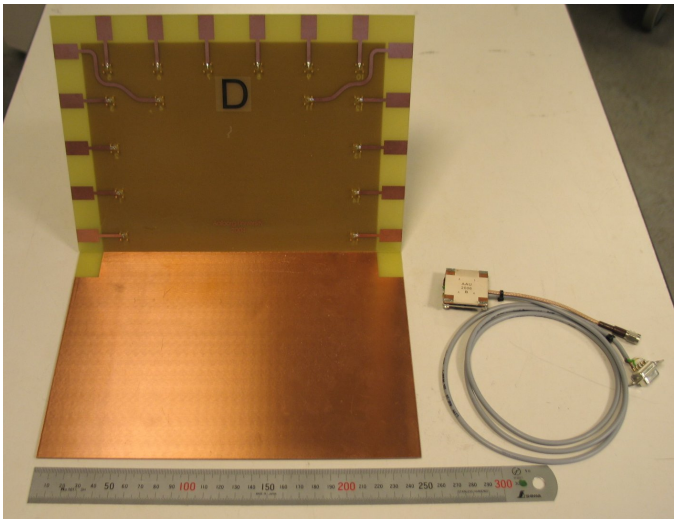

Fig. 6. The two arrays used at the MS's. To the right the body-worn array is seen at the end of a cable with the four antenna elements at the corners. The size of the array is about 3 cm by 3 cm. To the left the laptop-like array is seen, consisting of two planes connected at an angle of about 110°, with the plane on the table of size about 25 cm by 20 cm. Only four of the 16 elements along the edges are used, two at the top and one at each side of the "lid."

Two types of MS arrays are considered. The first type is designed to mimic an array built-in a laptop. Henceforth this is called a 'laptop array.' The other type of array consists of four patches at the corners of a square of size about 3 by 3 cm, which is mounted on the chest of a person. The two array types are illustrated in Fig. 6.

In total eight MS arrays are measured simultaneously and organized in four identical pairs of arrays, consisting of a body mounted array and a laptop array. Each pair was then associated with a different person. During the measurements described in the following the body mounted array is on the user's chest on a smock, except for the 'Free' measurement series where the user leaves the smock hanging on the chair, see below.

The measurement campaign was designed to involve four simultaneous users in different scenarios. However, the current work only uses a small part of the data obtained in the campaign, and hence the following only describes the parts relevant for the current work.

In the following only the data corresponding to one user, *i.e.*, one laptop and one body-mounted array are used. Three

Published in *IEEE Transactions on Wireless Communications, Vol. 8, No. 6, pp 3270-3277, June 2009.* DOI:10.1109/TWC.2009.081088

measurement scenarios are described below, where each of them was carried out at the table positions Rx01, Rx03, Rx05, as shown in Fig. 5. The different scenarios are

Static The MS remains static in location and the nearby environment does not change. During the measurements the user of the MS sits down at the table and simulate work at the "laptops" by "typing" or other types of movements nearby the MS.

ExtMov This type is carried out as the 'Static' type of measurement, except that during the measurement a person is walking around the table with the users.

Free All four users leave the laptop array on the table and the smock with the body worn device hanging on the chair. At the beginning of the measurement the users are standing behind the chair and starts walking; two of the users walk clockwise, while the other two walks counter-clockwise around the table.

IV. Data Processing

After the measurements were compensated for the system response, the MIMO impulse responses were processed in various ways. For the current work Doppler spectra need to be estimated. Instead of using a traditional fixed windowing of the data an apodization approach has been used where the data windowing depends on both the data and the frequency, as described in [10]. With this approach it is to some degree possible to avoid the common problem of trading resolution for leakage and essentially obtain the resolution of the rectangular window, but with significantly reduced leakage, as compared to that obtained with a traditional rectangular windowing [10]. With the current data a resolution of about 0.2 Hz is obtained and a level down to about -35 dB below the maximum can be estimated for a single channel. The narrowband Doppler spectra discussed in this work are obtained from estimated spectra of the wideband data.

Since the measurements are MIMO, a total of 16×32 spectra are obtained for each measurement, based on the 600 time-domain samples. With the purpose of reducing the estimation noise and the amount of data to analyze, the spectra obtained for elements of the same arrays have been averaged. By inspection the individual Doppler spectra were found to have the same overall shape, allowing averaging for reduced noise. For example, the $8 \times 4 = 32$ spectra obtained from all the channels between AP4 and elements of the first laptop array have been combined into a single spectrum with lower estimation noise. Alternatively, the resulting spectra may be seen as the average over different orientations and locations of the antenna elements.

V. Results

Fig. 7 compares the spectra for the 'Free' scenario to the similar results for the 'Static' scenario, both for the body mounted array. As expected, in all cases a strong component at 0 Hz is present in addition to components at all other frequencies at significantly lower levels and tending to a constant level. Although parts of the spectrum with constant level are due to estimation noise, the difference between the constant level and the peak at 0 Hz is an indication of the degree of channel changes. The difference of about 50 dB for the 'Static' scenarios is significantly higher than the about 30 dB found for the 'Free' scenarios. Note that all the spectra have the same general shape as the theoretical results in Fig. 4, although different parameters may be necessary for an optimum fit.

Comparing the curves for the Rx01, Rx03, and Rx05 positions differences of up to about 5 dB are found. It might be expected that the static part of the channel becomes more important with decreasing distance between the MS and the AP. Position Rx03 has the shortest distance to the AP but the spectrum for this measurement lies between the curves for the Rx01 and Rx05 positions, thus indicating that difference in the static and random part of the channel is not a simple function of the distance between the MS and the AP. Please also be reminded that the 0 Hz value in itself is a random number.

A similar grouping can be identified in Fig. 8 comparing the spectra for the 'ExtMov' and 'Static' scenarios, when the body mounted array is used. Again, the measurements with most activity in the environment forms a group with smaller distance between the constant level and the 0 Hz level, compared to the distance for the group with less channel activity. However, the difference between the two groups is less pronounced, about 10 dB compared to about 20 dB, which may be explained by the smaller degree of activity in these measurements.

The results discussed above are all for the body mounted array. Essentially similar comments can be made for the spectra for the laptop array. The spectrum bandwidths, however, are different. Fig. 9 gives an overview of the spectrum bandwidths, defined at the -20 dB level. It is evident that the bandwidths for the body mounted and laptop arrays are different, especially for the 'Free' measurements. During these measurements the smock with the body mounted array is hanging on the chair, and hence is below table height. The channel is significantly different from that of the laptop array which is on the table and perhaps less influenced by the persons walking by.

The measurements described above were designed to be realistic and at the same time allow numerous measurements. This, however, resulted in limitations regarding the accuracy of the estimated Doppler spectra. In order to better analyze spectra, it was decided to carry out a set of additional measurements with special focus on this issue. Unfortunately, the environment used for the measurements described above was not available and hence the extra measurements were instead carried out in a lab environment.

Two setups were used, a LOS where the Tx and Rx antennas were about 7 m apart, and a setup where the Tx end was moved about 3 m and hidden behind a bookshelf to create the NLOS scenario. Both the Tx and Rx antennas were omni-directional and mounted at a height of about 1 m above the floor. For the LOS setup four measurements were carried out:

Stand: During the measurement a person is standing in the middle on the path connecting the Tx and the Rx. The person is not moving and no other activity takes place in the laboratory.

Slow: Similar to "Stand" except that the person is walking

Published in *IEEE Transactions on Wireless Communications, Vol. 8, No. 6, pp 3270-3277, June 2009.* DOI:10.1109/TWC.2009.081088

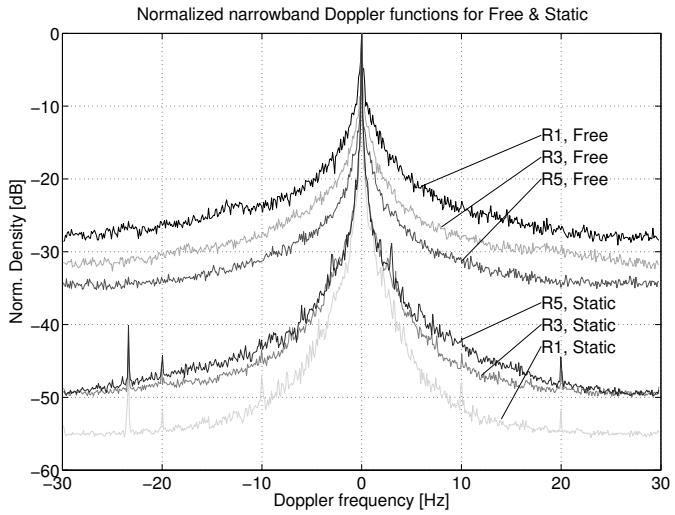

Fig. 7. Doppler spectra for body mounted arrays in the 'Free' scenario with people walking close by, and the 'Static' scenario with little activity in the channel. The curves are normalized to have a peak of 0 dB.

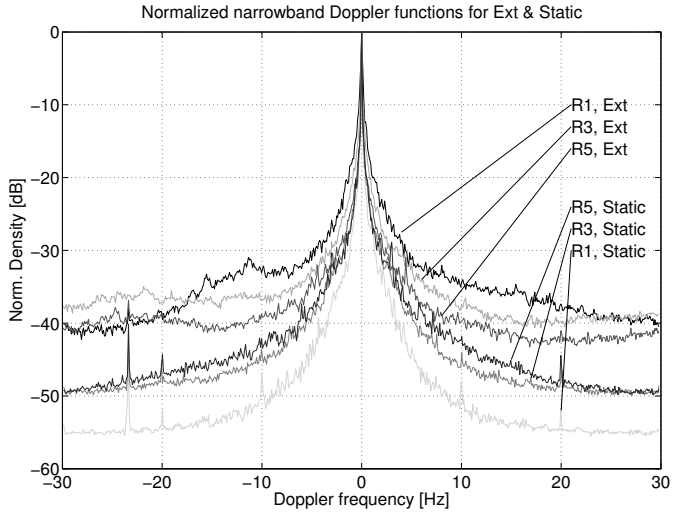

Fig. 8. Doppler spectra for body mounted arrays in the 'ExtMov' scenario where a single person is walking near the user, and the 'Static' scenario with little activity in the channel. The curves are normalized to have a peak of 0 dB.

slowly back and forth an about 2 m section centered between the Tx and Rx.

Fast: Same as "Slow", but with the person walking fast.

Corridor: The person is walking at medium speed in a corridor next to the laboratory, about 5 m from the LOS path. The corridor runs in parallel to the laboratory and they are connected by two large openings.

For the NLOS setup the same four measurements were made, with the only difference being that the Tx antenna was moved compared to the LOS setup.

All the measurements were 60 s long, corresponding to 3600 channel samples. Using the same approach as described above, the Doppler spectra were then estimated. Due to the larger number of samples the frequency resolution is of the order 0.02 Hz. The results given below are for a single channel, *i.e.*, no averaging was done.

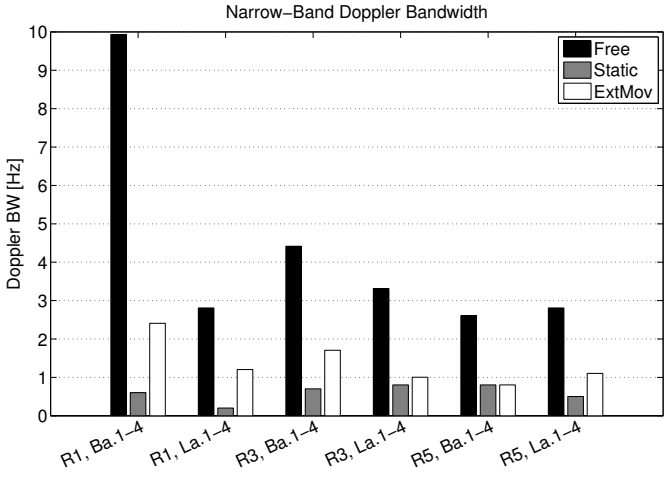

Fig. 9. Bandwidth of Doppler spectrum at the -20 dB level for all combinations of 'Free', 'Static', 'ExtMov' scenarios for both the body mounted ('Ba' labels) and laptop arrays ('La' labels).

The observed spectra are composed of components due to the static and random parts of the channel. Whereas the static parts only result in components at 0 Hz, the random changes in the channel result in components both at 0 Hz and at other frequencies, as mentioned in Section II-D.

As described above, the channel was first measured as completely static, then again with some random channel changes. By comparing the resulting spectrum estimates, the parts due to the random scatteres are revealed. Unfortunately, the spectrum estimate is not perfect and to some degree the estimation noise depends on the spectrum. This makes a direct comparison difficult.

The spectra for the four types of measurements in the LOS case are shown in Fig. 10. As expected, the curve for the "Stand" measurement has a very narrow peak at 0 Hz with a "skirt" in the region ± 2 Hz and a "floor" at about -67 dB. The imperfect spectrum is resulting from both system phase noise and spectral leakage of the estimation method. Also to be noted are two peaks at ± 1 Hz which are due to spurious signals in the system.

Compared to the "Stand" measurement, activity in the corridor leads to essentially the same spectrum, which is expected since the changes presumably are in a place from where only relatively weak signal components are received.

Activity in the LOS changes the spectrum, but surprisingly the fast movements changes the spectrum only slightly (but noticeably) over that for the slow movements. Note that the apparent change in the level of the "floor" is explained by increased spectral leakage arising from the extra components near 0 Hz. These components introduced by the moving person have a magnitude of about -35 dB near 0 Hz, decreasing to about -45 to -40 dB at ± 1 Hz.

It is interesting to compare these results with the similar ones for the NLOS measurements, shown in Fig. 11. The spectra for the "Fast" and "Slow" cases are more similar in the NLOS than in the LOS case, but the spectra for the "Slow" case in the LOS and NLOS scenarios are very alike.

Published in *IEEE Transactions on Wireless Communications, Vol. 8, No. 6, pp 3270-3277, June 2009.* DOI:10.1109/TWC.2009.081088

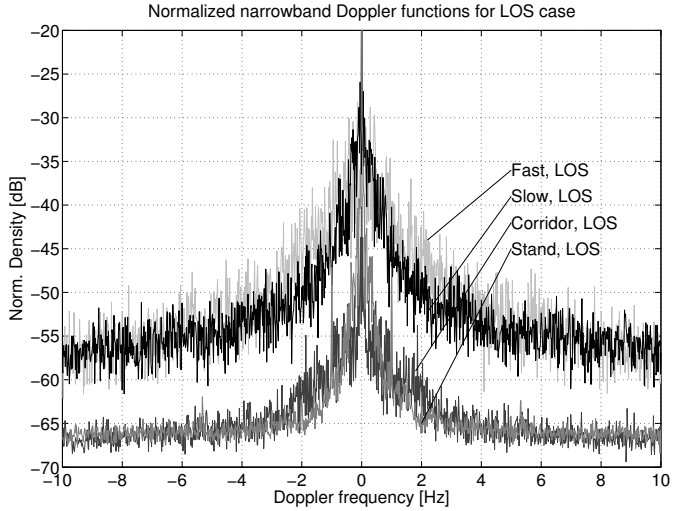

Fig. 10. Doppler spectra for laboratory measurements, LOS case. Note that all curves are normalized to have a peak of 0 dB, but the spectrum is cut at an upper y-axis limit of -20 dB.

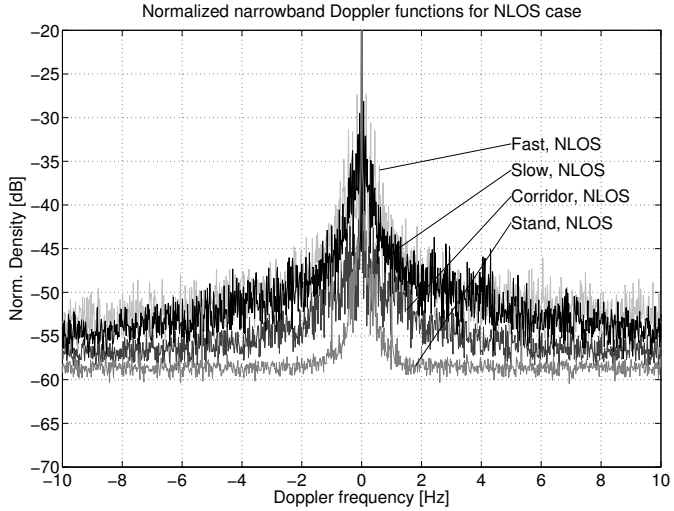

Fig. 11. Doppler spectra for laboratory measurements, NLOS case. Note that all curves are normalized to have a peak of 0 dB, but the spectrum is cut at an upper y-axis limit of -20 dB.

Without a dominating LOS component the activity in the corridor results in a noticeable change in the spectrum compared to the "Stand" case.

As discussed above, the spectrum for the "Stand" case is not the ideal single peak at 0 Hz. The spectra for the LOS and NLOS cases are practically identical down to a level about -55 dB below which the curve for LOS tends to a lower level. The phase noise level is the same for the two cases but has larger impact on the NLOS case due to the larger dispersion in this channel.

VI. Conclusion

In the current work the Doppler spectrum for fixed transceivers in an environment with randomly moving scatterers is analyzed. The spectrum is derived theoretically and some special cases are detailed, namely a scatterer moving in one direction, a scatterer moving in many directions, both for a constant scattering cross section and also the more realistic case of non-uniform scattering cross section. The theoretical spectra are compared to results from measurements in realistic scenarios using both arrays on a laptop and mounted on a user's chest. Wideband measurements were made in an indoor open office type environment with random changes in the channel nearby the mobile device. The spectra estimated from the measurements have the same overall shape predicted by the theory for the non-uniform scattering cross section, with a strong component at 0 Hz in addition to components with a level decreasing with frequency. Spectrum bandwidths of 1-9 Hz were observed at a -20 dB level, depending on the degree of activity in the environment. The components due to the non-static parts of the channel are relatively weak and difficult to measure, and furthermore depends on the environment. In a laboratory environment most of the components due to random changes were estimated to be more than 30 dB below the 0 Hz component.

References

[1] R. J. C. Bultitude, "Measurement, characterization and modeling of indoor 800/900 MHz radio channels for digital communications," *IEEE Communications Magazine*, vol. 25, no. 6, pp. 5–12, Jun. 1987.

[2] S. J. Howard and K. Pahlavan, "Doppler spread measurements of indoor radio channel," *Electronics Letters*, vol. 26, no. 2, pp. 107–109, Jan. 1990.

[3] S. Thoen, L. V. der Perre, and M. Engels, "Modeling the channel time-variance for fixed wireless communications," *IEEE Communications Letters*, vol. 6, no. 8, pp. 331–333, Aug. 2002.

[4] A. S. Akki and F. Haber, "A statistical model of mobile-to-mobile land communication channel," *IEEE Transactions on Vehicular Technology*, vol. VT-35, no. 1, pp. 2–7, Feb. 1986.

[5] A. G. Zajić and G. Stüber, "Space-time correlated mobile-to-mobile channels: Modelling and simulation," *IEEE Transactions on Vehicular Technology*, vol. VT-57, no. 2, pp. 715–726, Mar. 2008.

[6] R. H. Clarke, "A statistical theory of mobile radio reception," *Bell System Technical Journal*, vol. 47, pp. 957–1000, 1968.

[7] A. Ishimaru, *Electromagnetic Wave Propagation, Radiation, and Scattering*. Prentice Hall, 1991.

[8] I. Gradsteyn and I. Ryzhik, *Table of Integrals, Series, and Products*. Academic Press, San Diego, 1980.

[9] J. Ø. Nielsen and J. B. Andersen, "Indoor MIMO channel measurement and modeling," in *The Proceedings of the International Symposium on Wireless Personal Multimedia Communications (WPMC'05)*, 2005, pp. 479–483.

[10] P. Stoica and R. Moses, *Spectral Analysis of Signals*. Pearson Prentice Hall, 2005.

Published in *IEEE Transactions on Wireless Communications, Vol. 8, No. 6, pp 3270-3277, June 2009.* DOI:10.1109/TWC.2009.081088

Jørgen Bach Andersen (M'68–SM'78–F'92–LF'02) received the M.Sc. and Dr.Techn. degrees from the Technical University of Denmark (DTU), Lyngby, Denmark, in 1961 and 1971, respectively. In 2003 he was awarded an honorary degree from Lund University, Sweden. From 1961 to 1973, he was with the Electromagnetics Institute, DTU and since 1973 he has been with Aalborg University, Aalborg, Denmark, where he is now a Professor Emeritus.

He has been a Visiting Professor in Tucson, Arizona, Christchurch, New Zealand, Vienna, Austria, and Lund, Sweden. From 1993-2003, he was Head of the Center for Personkommunikation (CPK), dealing with modern wireless communications. He has published widely on antennas, radio wave propagation, and communications, and has also worked on biological effects of electromagnetic systems. He was on the management committee for COST 231 and 259, a collaborative European program on mobile communications. Professor Andersen is a Life Fellow of IEEE and a former Vice President of the International Union of Radio Science (URSI) from which he was awarded the John Howard Dellinger Gold Medal in 2005.

Jesper Ødum Nielsen received his master's degree in electronics engineering in 1994 and a PhD degree in 1997, both from Aalborg University, Denmark. He is currently employed at Department of Electronic Systems at Aalborg University where main areas of interests are experimental investigation of the mobile radio channel and the influence on the channel by users. He has been involved in channel sounding and modeling, as well as measurements using the live GSM network. In addition he has recently been working with handset performance evaluation based on spherical measurements of handset radiation patterns and power distribution in the mobile environment.

Gert Frølund Pedersen was born in 1965. He received the B.Sc. E. E. degree, with honour, in electrical engineering from College of Technology in Dublin, Ireland, and the M.Sc. E. E. degree and Ph. D. from Aalborg University in 1993 and 2003. He has been employed by Aalborg University since 1993 where he is now Professor for the Antenna and Propagation group. His research has focused on radio communication for mobile terminals including Antennas, Diversity systems, Propagation and Biological effects and he has published more than 50 peer reviewed papers and holds 16 patents. He has also worked as consultant for developments of antennas for mobile terminals including the first internal antenna for mobile phones in 1994 with very low SAR, first internal triple-band antenna in 1998 with low SAR and high efficiency, and lately various multi antenna systems rated as the most efficient on the market. He has been one of the pioneers in establishing over-the-air measurement systems. The measurement technique is now well established for mobile terminals with single antennas and he is now chairing the COST2100 SWG2.2 group with liaison to 3GPP for over-the-air test of MIMO terminals.

Gerhard Bauch received the Dipl.-Ing. and Dr.-Ing. degree in Electrical Engineering from Munich University of Technology in 1995 and 2001, respectively, and the Diplom-Volkswirt degree from FernUniversitaet Hagen in 2001. In 1996, he was with the German Aerospace Center (DLR), Oberpfaffenhofen, Germany. From 1996-2001 he was member of scientific staff at Munich University of Technology (TUM). In 1998 and 1999 he was visiting researcher at AT&T Labs Research, Florham Park, NJ, USA. In 2002 he joined DOCOMO Euro-Labs, Munich, where he has been manager of the Advanced Radio Transmission Group. In 2007 he was also appointed Research Fellow at DOCOMO Euro-Labs. Since 2009 he is a Full Professor at the Universitaet der Bundeswehr Munich. From 2003-2008 he was also an adjunct professor at Munich University of Technology. Furthermore, he lectured as guest professor at the University of Udine, Italy, and the Alpen-Adria University Klagenfurt, Austria. He received best paper awards of the European Personal Mobile Communications Conference (EPMCC) 1997 and IEEE Globecom 2008, the Texas Instruments Award 2001 of TUM, the Award of the German Information Technology Society (ITG in VDE) 2002 (ITG Foerderpreis) and the Literature Award 2007 of the German Information Technology Society (ITG in VDE). He has (co-)authored a textbook on Contemporary Communications Systems as well as more than 100 scientific papers in major journals and international conferences. His research interests include channel coding and modulation, turbo processing, multihop transmission, multiple access and various aspects of signal processing in multi-antenna systems (MIMO).

Guido Dietl (S'01–M'07) received the Dipl.-Ing. and Dr.-Ing. degrees (both summa cum laude) in Electrical Engineering from the Technische Universität München (TUM, Munich University of Technology), Munich, Germany, in 2001 and 2006, respectively.

He has been with the TUM from 2001 to 2006 where he was working as a Research Engineer on reduced-rank signal processing in Krylov subspaces and on its application to wireless multiuser communications. In Winter 2000/2001 and Summer 2004, he was a Guest Researcher at Purdue University, West Lafayette, IN, USA. In Fall 2005, he visited the Australian National University (ANU) in Canberra, ACT, Australia. He joined DOCOMO Communications Laboratories Europe GmbH (DOCOMO Euro-Labs), Munich, Germany, in 2006, where he is currently Senior Researcher of the Wireless Technologies Research Group.

Dr. Dietl received the VDE Award for his Diploma thesis in 2001, the Kurt Fischer Award of the TUM for his dissertation in 2007, and the Förderpreis der ITG 2007 of the Informationstechnische Gesellschaft (ITG, Information Technology Society in VDE), also for his dissertation.

His main research interests are multiuser multiple-input multiple-output (MIMO) communications, wireless relay networks, iterative (Turbo) detection, reduced-rank signal processing, and numerical linear algebra.

Published in *IEEE Transactions on Wireless Communications, Vol. 8, No. 6, pp 3270-3277, June 2009.* DOI:10.1109/TWC.2009.081088